A Density Functional Theory Study on the Intramolecular Proton Transfer in the Enzyme Carbonic Anhydrase

Hui Chen, Shuhua Li,* and Yuansheng Jiang

Department of Chemistry, Institute of Theoretical and Computational Chemistry, Lab of Mesoscopic Materials Science, Nanjing University, Nanjing 210093, PRC

Received: August 19, 2002; In Final Form: January 23, 2003

Density functional calculations are used to explore the mechanism of the intramolecular proton transfer (PT) from Zn-bound H_2O to the proton acceptor His64 in the enzyme carbonic anhydrase (CA). By performing free and restricted geometry optimizations on the model system $(Im_3)_3Zn^{2+}\cdots(OH_2)_3\cdots Im$ (Im is imidazole), we determine the PT potential energy profiles under three conditions: (a) without geometric restrictions, (b) with the proton donor−acceptor distance fixed, and (c) with the relative orientation of the imidazole acceptor fixed. The latter two circumstances are invoked to mimic the effect of the protein framework on the PT energy surface. Our calculations indicate that the PT process involves a concerted mechanism under all three of these conditions. If we take into account the effects of the protein framework, the protein electrostatic environment, and zero-point vibrational energies altogether, we obtain a reasonable estimate of ∼7 kcal/mol for the PT barriers in both hydration and dehydration directions, which agree well with the experimental values. In addition, the influence of the nearby residues or surrounding water molecules on the PT energy surface is modeled by adding two side waters to the water chain of the model system. Calculations suggest that if the hydrogen bond interaction between the side water (or any other residue) and the water in the water bridge is sufficiently strong a two-step proton transfer mechanism is favored; otherwise, the intramolecular proton transfer may still occur in a concerted way.

1. Introduction

The carbonic anhydrase (CA) is the first enzyme to be found containing zinc ion.[1] It catalyzes the hydration of CO_2 to form HCO_3^- and H^+, i.e., $CO_2 + H_2O = HCO_3^- + H^+$. The active site of CA consists of a four-coordinated zinc ion with three histidine imidazole groups and one water molecule bound to the zinc. The zinc ion is coordinated by two ϵ-nitrogen atoms, one δ-nitrogen atom, and one oxygen atom of water to complete the tetrahedral geometry. The image of the active site of the human carbonic anhydrase (the most efficient one in the seven known isoenzymes of carbonic anhydrase found in higher vertebrates),[2] as determined by X-ray diffraction, is shown in Figure 1.[3]

The catalytic mechanism of CA has been extensively studied both experimentally[4−21] and theoretically.[22−35] Now the generally accepted mechanism consists of the following three steps.

$$EZnOH_2 = EZnOH^- + H^+ \quad (1)$$

$$EZnOH^- + CO_2 = EZnHCO_3^- \quad (2)$$

$$EZnHCO_3^- + H_2O = EZnOH_2 + HCO_3^- \quad (3)$$

Here E stands for the enzyme. Experiments have shown that the deprotonation step of eq 1 is rate-determining in the catalytic cycle of CA.[7] Furthermore, the deprotonation step is generally considered to include (1) the intramolecular proton transfer (PT) from Zn-bound H_2O to the remote group His64 and (2) the intermolecular PT from His64 to the buffer molecule and then to the solvent.[23] The intramolecular proton transfer is known to be the rate-limiting step[4,5] at high buffer concentrations, and the proton transfer into the medium is rate-limiting at low buffer concentrations.[6]

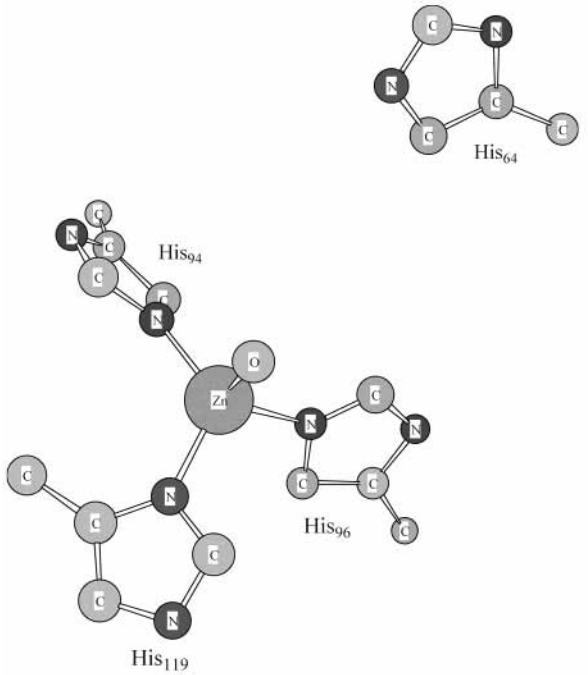

Figure 1. Schematic representation of the active site in HCA (all hydrogens are neglected).

Although there is general agreement about the overall mechanism involved in the catalytic process of CA, the picture of the proton transfer process has not yet been fully understood. Theoretical calculations suggested that the intermolecular PT from the protonated His64 to a buffer molecule (and then to the solvent) is a low-energy process,[23,26] but the mechanism of the intramolecular PT process is still a question to be resolved.

10.1021/jp026788k CCC: $25.00
Published on Web 05/17/2003

SCHEME 1

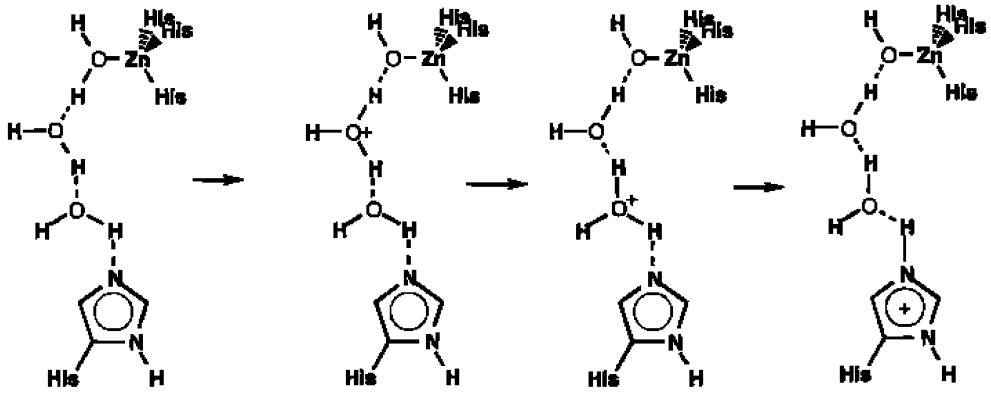

A general accepted mechanism for the intramolecular PT step has been given by Venkatasubban and Silverman.[8] In this mechanism, two water molecules form a "water bridge" to transfer one proton from zinc-bound water to His64. X-ray diffraction results show that the Zn^{2+} ion is ~7.8 Å from His64.[9] Therefore, there are possibly as many as three water molecules between them, and consequently, the existence of this water bridge is possible. Recent molecular dynamics studies[35] on CA also revealed that the most frequently appearing water bridge contains three water molecules. Of course, the protein framework and surrounding protein electrostatic environment may have a significant influence on the PT energy surface. In addition, the residues near the active site such as Thr199, Tyr7, Glu106, etc., might also influence to some extent the proton transfer process.

To gain insight into how a proton transfers from Zn-bound H_2O to His64 through a water bridge, several theoretical studies have been carried out,[23,26,32,34,35] among which two possible PT mechanisms have been investigated. The first one is a step-by-step proton relay mode, which is shown in Scheme 1. The second mechanism involves a concerted process, in which at least two protons transfer at one time. Liang and Lipscomb[23] studied a model system with all imidazole ligands replaced with ammonia molecules by using semiempirical and ab initio methods. They obtained a concerted mechanism with an energy barrier of 34 kcal/mol for the four-coordinated zinc complex, which is too high in comparison with the experimental value of 7.8 kcal/mol[19] for the hydration (away from zinc) direction. It is worthwhile to point out that the experimental barriers are actually free energy barriers obtained from fitting to Marcus theory. Hence, there is some uncertainty in comparing electronic structure energy barriers with the experimental values. Merz et al.[26] used the semiempirical AM1 method and a more realistic model. Their calculations showed that a concerted process has a barrier height of 18 kcal/mol, which is still a little high in comparison with experiment.

Voth and Lu[32] carried out a detailed investigation on the stepwise PT process by using ab initio methods. They used the double-ζ basis set for geometry optimizations and built several model systems with histidine residues represented by different substituents. They investigated the effects of various factors such as the protein geometry constraints and the number of hydrogen-bonded water molecules on the PT energetics. It was found that a single proton transfer in the dehydration direction (from His64 to the adjacent H_2O) has a barrier of ~8−10 kcal/mol, which agrees well with experiment, while the barrier of a single proton transfer in the hydration direction is very sensitive to the histidine ligand bonding around the Zn ion. Their calculations also revealed that a proton transfer between Zn-bound water and His64 requires a certain hydrogen bond formation in the active site. Thus, their studies gave results that were more quantitative than those reported earlier; however, we notice that the concerted PT mechanism was not studied in this work.

Very recently, Isaev and Scheiner[34] used ab initio and density functional theory (DFT) calculations to study the proton transfer process in the $(NH_3)_3Zn^{2+}\cdots(OH_2)_3\cdots NH_3$ model system. Their calculations suggested that the most energetically accessible pathway for proton transfer from the Zn-bound water to the terminal NH_3 group is a concerted process wherein three protons are simultaneously in flight from one molecule to the next along the water chain. They also found that peripheral hydrogen bonds, formed between the waters of the water bridge and side waters, and the relative orientation of the terminal NH_3 acceptor have a substantial effect upon the PT process. Because they used NH_3 to model the imidazole of histidine and employed the Hartree−Fock (HF) method with the 6-31G basis set for geometry optimizations, their results should not be considered quantitative in describing the proton transfer barrier in CA.[34]

Despite the encouraging insights gained for the mechanism of proton transfer in CA, a theoretical study using a realistic model and a high accurate quantum chemistry method to explore the PT potential energy profiles under various situations is still desirable, which is the goal of this paper. We chose DFT as our theoretical method because its computational scaling with the size of the system is approximately the same as that of the HF method, but the accuracy of the best DFT method is believed to be comparable to that of the MP2 method for general compounds.[36] Thus, we can optimize the geometries of large models that are being considered, which cannot be done with other available correlation methods. In comparison with previous ab initio studies, in which only double-ζ basis sets were employed for geometry optimizations, we use a larger basis set of double-ζ plus polarization (DZP) quality for full or partial geometry optimizations. Since Voth and Lu had shown that replacing histidine ligands with ammonia molecules is not likely to be quantitatively valid,[32] we use an imidazole (Im) molecule to model a histidine ligand in all calculations. Thus, the primary model system we choose for the active site of CA is $(Im_3)_3Zn^{2+}\cdots(OH_2)_3\cdots Im$ (called the three-water model, as shown in Figure 2), which should be adequate for studying the intramolecular PT process in CA. With the selected method and model, the PT barrier and mechanism under several circumstances are studied, and the structures of the relevant species involved in the PT process are determined. For example, the effect of the protein backbone on the PT barrier and mechanism is approximately studied through constraining some relevant freedoms of the model system. To probe the effect of the residues near the active site, two side waters are added to the

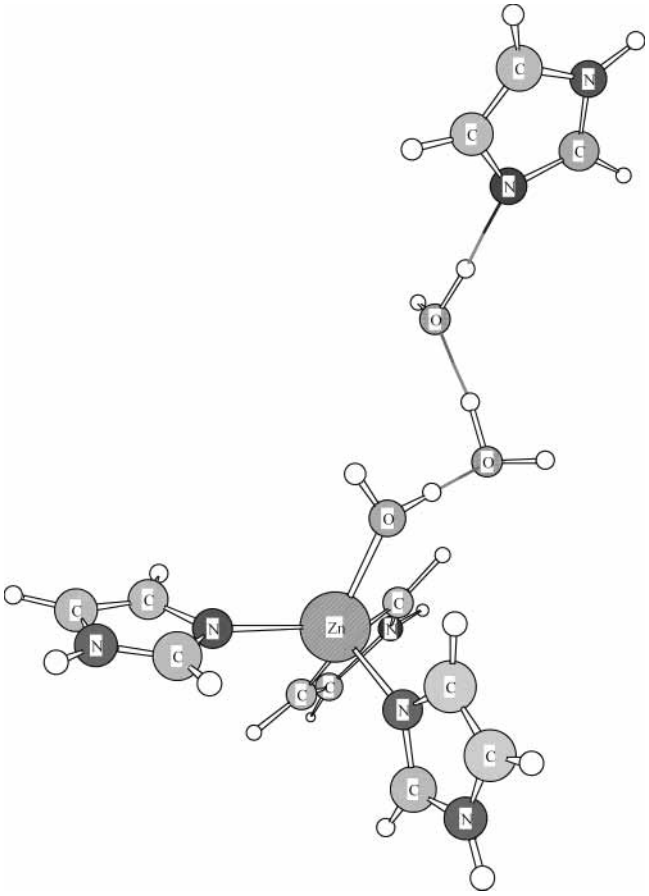

Figure 2. Three-water model of the active site of CA.

water chain of the model system to form a new model for study. Our calculations show that the proton transfer along the water shuttle is most likely to occur in a concerted way, except that the hydrogen bond between the side water and the bridged water is quite strong, which may lead to a two-step mechanism.

2. Computational Details

All the calculations have been performed with the Gaussian98 package.[37] Density functional theory was employed with the three-parameter hybrid exchange functional of Becke and the Lee, Yang, and Parr correlation functional (B3LYP). For zinc, the relativistic effective core potential (ECP) was employed in all B3LYP calculations. The basis set for zinc is a modified LANL2DZ double-ζ basis set plus an f-type polarization function,[38] in which the two 4p functions of the standard LANL2DZ have been replaced with the optimized 4p functions from Couty and Hall.[39] For all the other atoms, two basis sets are used. The 6-31G(d,p) basis set (basis set I) is employed for all geometry optimizations; then the energetics of potential energy profiles are obtained by performing single-point calculations with the 6-31++G(d,p) basis set (basis set II). Full or restricted geometry optimizations have been performed to determine the structures of reactants, intermediates, transition states, and products in the PT process. For freely optimized species, a frequency calculation with basis set I is carried out to calculate zero-point energies (ZPEs) and verify whether it is a minimum or a transition state. To consider the effects of the protein backbone and the residues near the active site on the proton transfer process, the model system with some relevant freedoms fixed or a modified model system, as described in the next section, is employed.

TABLE 1: Relative Energies (kcal/mol) of Species Related to the Three-Water Model under Various Conditions (ZPE Corrections Calculated with Basis Set I)

	model A[a]		model B[b]		model C[c]	
species	E_o	E_o + ZPE	E_o	E_o	E_o	E_o ($\epsilon = 2$)
reactant	0.0	0.0	0.0	0.0	0.0	0.0
TS	2.7	−1.7	3.4	5.0	13.4	11.0
product	−5.37	−5.2	−5.5	−5.1	0.2	−0.2

[a] Model A is the freely optimized model. [b] Model B is the model where R(D−A) = 6.6 Å (column 4) or 7.0 Å (column 5). [c] Model C is the model with the relative orientation of His64 of the imidazole fixed at positions as determined in the X-ray structure. The gas phase results are listed in column 6, and the results with a dielectric constant ϵ of 2 are included in column 7.

Before the selected DFT method is applied to calculate the PT potential energy profiles, it is important to judge its accuracy by applying it to relevant small systems, where more accurate theoretical calculations or experimental values are available for calibration. Here we apply the B3LYP method to calculate the proton transfer barriers in two typical hydrogen-bonded systems, the $H_5O_2^+$ system and the formic acid dimer system. For the $H_5O_2^+$ system, the proton transfer barrier from B3LYP calculations with the 6-31++G(d,p) basis set is 0.3 and 0.9 kcal/mol lower than the corresponding value obtained at the MP2/aug-cc-pvtz level at two important distances, R(O−O), of 2.6 and 2.8 Å, respectively. In the formic acid dimer, B3LYP/6-31++G(d,p) calculations give a double proton transfer barrier of 5.8 kcal/mol, 2.2 kcal/mol lower than the value (8.0 kcal/mol) calculated at the MP2/6-31++G(d,p) level. Branko[40] also studied the PT barrier in this system in detail by using MP2 and other correlation methods with even larger basis set. The B3LYP/6-31++G(d,p) result presented here is found to be ∼2−3 kcal/mol lower than his results. To summarize the results given above, one can see that the accuracy of the B3LYP/6-31++G(d,p) method in calculating the PT barrier depends to some extent on the number of protons involved in the PT process. For the CA system that is being studied, if the PT process involves a concerted motion of three protons, the B3LYP method with the 6-31++G(d,p) basis set should be able to compute the PT barrier quite accurately, being ∼2−3 kcal/mol lower than those from higher-level calculations.

3. Results and Discussion

3.1. Fully Optimized Model. Without geometric restrictions, our optimizations on the model system lead to a reactant **1**, the zinc-bound water species, a product **3**, the zinc-bound hydroxide species, and a well-defined transition state (TS) **2**. The IRC calculations indicate that TS **2** truly connects **1** and **3**. From the obtained structures shown in Figure 3, one can see that in TS **2** two protons are almost in the middle of two neighboring oxygen atoms, and one proton lies between the imidazole nitrogen (His64) and its adjacent oxygen atom. Thus, this transition state involves a concerted movement of three protons. The calculated distance between the zinc ion and the imidazole nitrogen (His64) is 7.73 Å for **1**, 8.38 Å for **2**, and 7.78 Å for **3**, being very close to the distance of 7.8 Å observed in the HCA X-ray structure.[9] When the proton transfer reaction goes from **1** to **3**, the Zn−O distance decreases from 2.02 to 1.93 Å, in accord with the electrostatic attraction between the positive zinc ion and the negative hydroxide group in **3**. Following the step-by-step proton transfer mechanism, we cannot find the corresponding intermediates. The energies of **1**−**3** calculated with basis set II are listed in Table 1. Without ZPE corrections, the calculated energy barrier from **1** to **3** is 2.68 kcal/mol, and

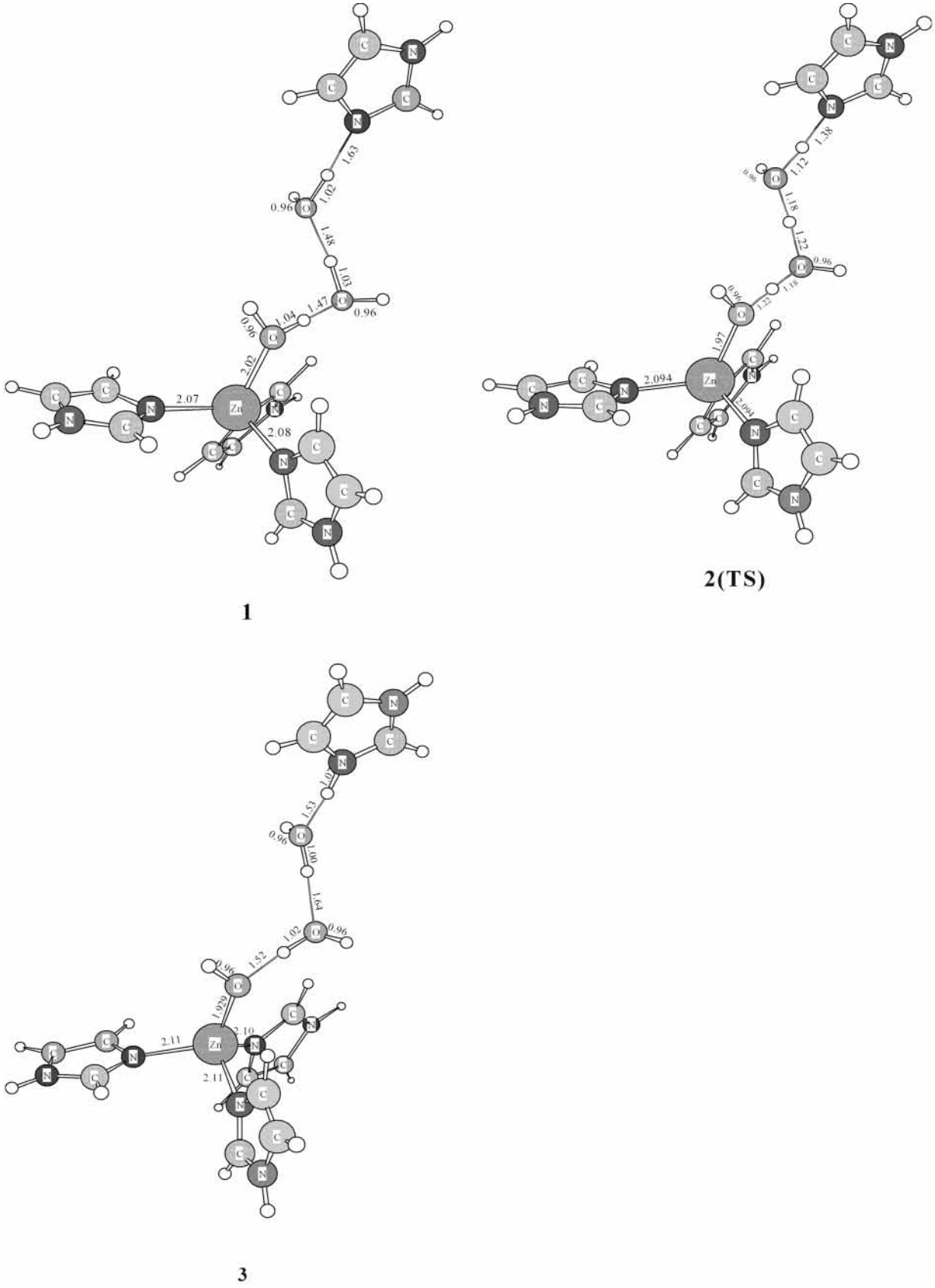

Figure 3. B3LYP-optimized structures related to the freely optimized three-water model.

the reverse process has a barrier of 8.05 kcal/mol. Since the ZPE corrections (calculated with basis set I) would lower the PT barrier in the hydration direction by ~4.37 kcal/mol (as shown in Table 1), the transition state is slightly lower in energy than the reactant **1**. Even if we consider that the PT barrier calculated from B3LYP is often underestimated by ~2−3 kcal/mol,[40] the estimated PT barrier in the hydration (or dehydration) direction is still significantly lower than that of the experimental value. In summary, when the freely optimized model system is employed, our calculations indicate

that the concerted PT process is almost energetically spontaneous. This result is consistent with that given by Isaev and Scheiner,[34] who performed full geometry optimizations on the $(NH_3)_3Zn^{2+}\cdots(OH_2)_3\cdots NH_3$ model system.

Of course, the freely optimized model system deviates from the real enzyme in many ways. There are several important factors that may have a substantial effect on the PT energetics. First, the structure of the enzyme actually constrains the locations of the remote His64 group (and thus the positions of the water molecules in the shuttle), as shown in the HCA X-ray structure.[9] Second, the residues near the active site might form hydrogen bonds to the waters in the water chain and, thus, might have a significant effect on the PT energy surface, as revealed by Voth and Lu. Third, the protein electrostatic environment might influence to some extent the PT surface. In the following, we will probe the effect of geometric restrictions on the PT process by using the model system with (a) the proton donor−acceptor (D−A) distance fixed and (b) the relative orientation of the terminal imidazole acceptor fixed. The effect of the nearby residues will be investigated by adding two side waters to the water chain of the model system. In addition, the effect of the protein electrostatic environment on the PT barrier will be examined by doing polarized continuum model calculations.

3.2. Model with the Donor−Acceptor Distance Fixed. Although the distance between the zinc ion and the imidazole nitrogen (His64) obtained from free optimizations agrees well with that of the X-ray structure, the donor−acceptor distance, between the Zn-bound oxygen atom and the imidazole nitrogen (His64), is much shorter than the one in the X-ray structure. This is because under the free optimization condition the imidazole acceptor deviates significantly from the position of His64 in the X-ray structure. This short proton donor−acceptor distance may decrease the PT barrier as demonstrated previously by Voth and Lu.[32] In the fully optimized reactant **1**, the donor−acceptor distance is 5.85 Å, whereas in the crystal structure, the distance is 7.50 Å. To demonstrate the effect of the donor−acceptor distance on the PT process, we froze this distance at 6.60 and 7.00 Å, respectively, and leave all the other freedoms to be optimized. At these two selected distances, we still obtain the well-defined transition state representing the concerted motion and the two minima structurally similar to **1** and **3**. Without ZPE corrections, the calculated energy barrier (with basis set II) for the hydration direction with a D−A distance of 6.60 Å is 3.4 kcal/mol, and the reverse process has a barrier of 8.9 kcal/mol (collected in Table 1). When the D−A distance is increased to 7.0 Å, the barrier for the hydration direction increases to 5.0 kcal/mol and the barrier of the reverse process increases to 10.1 kcal/mol. This result clearly shows the influence of the donor−acceptor distance on the barrier of the concerted PT process. The similar effect was obtained by Voth and Lu[32] in studying the stepwise PT process.

3.3. Model with the Relative Orientation of the Terminal Imidazole Constrained. Besides the D−A distance, the orientation of His64 relative to the Zn−O axis between Zn and its bound water molecule should have an important effect in the enzymatic control of the PT process. With a relatively smaller model system, Isaev and Scheiner[34] have observed this effect from their calculations. Here with the current model system, we investigate the PT barrier under circumstances in which the relative orientation of the terminal imidazole is fixed at positions as determined in the X-ray structure. To do so, we constrain the distance between the nitrogen atom (N_4) of the terminal imidazole and the Zn-bound oxygen atom (O_1), the $Zn-O_1-N_4$ angle, and the $N_1-Zn-O_1-N_4$ dihedral angle to the corresponding experimental values in the X-ray structure: $R(O_1-N_4) = 7.50$ Å, $Zn-O_1-N_4$ angle $= 93.87°$, and $D(N_1-Zn-O_1-N_4) = -175.07°$ (as illustrated in Figure 4). For reducing the computational cost, the internal freedoms of three Zn-bound imidazole groups are frozen at values determined in the freely optimized reactant **1** because their values change little during the PT process within the freely optimized model system, i.e., from **1** to **3**. By fixing the freedoms described above and optimizing all other freedoms, we successfully locate two species, **4** and **6**, representing the PT reactant and product, respectively, and a concerted transition state **5** connecting these two species, as shown in Figure 4. The structure of **5** clearly shows that the transfer of three protons is not precisely synchronous. From the reactant to the transition state, the transfer of H_1 is almost complete, the transfer of H_2 is approximately half complete, and the H_3 transfer is still in the early stages. After the reaction crosses the transition state, the transfer of H_3 dominates and the H_2 transfer continues. Comparing the structure of **5** with that of the freely optimized transition state **2**, one can see that the degree of being concerted of the proton transfer mode decreases significantly in the transition state **5**. On the other hand, the PT barrier is 13.4 kcal/mol in the hydration direction and 13.2 kcal/mol in the dehydration direction (Table 1). The barrier obtained here in either direction is significantly higher than the corresponding value obtained in the previous subsection, in which only the D−A distance is fixed to be 6.60 and 7.00 Å, respectively. In addition, from the current model, the hydration direction barrier is now very close to the dehydration direction barrier, while from the model with only the D−A distance fixed, the hydration direction barrier is ∼5 kcal/mol lower than the dehydration direction barrier in both distances that were studied. Obviously, there are two factors responsible for this consequence. One is the larger D−A distance (7.50 Å) used in the current model, which should increase the PT barrier in both directions relative to R(D−A) values of 6.60 and 7.00 Å. Another factor, the orientation of the terminal imidazole relative to the $Zn-O_1$ bond, should be responsible for the closeness of the PT barrier in both directions.

It is also important to probe the effect of the protein electrostatic environment on the PT barrier, as addressed previously.[32] To do so, one usually treats the protein environment as a dielectric continuum (the dielectric constant being typically 2−4) and employs self-consistent reaction field methods. With the current model, we run polarized continuum model (PCM) calculations on three species (**4**−**6**) obtained above with a dielectric constant ϵ of 2. We find that the PT barrier decreases to 11 kcal/mol for the hydration direction and to 11.2 kcal/mol for the dehydration direction (Table 1).

If we consider the fact that the effect of ZPE would lower the PT barrier in either the hydration or dehydration direction by ∼4 kcal/mol (as shown in Table 1), we obtained a reasonable estimate of ∼7 kcal/mol for the PT barrier in both directions. Even if the underestimation (∼2−3 kcal/mol) of the used B3LYP in calculating the PT barrier is considered, one can see that the estimated PT barriers in both directions presented here agree well with the experimental values. A comparison of the results obtained from this subsection with those from the previous two subsections reveals that the geometric constraints enforced by the protein framework and the surrounding electrostatic environment on the model system are crucial for bringing the calculated PT barriers into the range of the experimental values.

3.4. Model with the Two "Side" Water Molecules Added. Previous studies showed that the residues near the active site

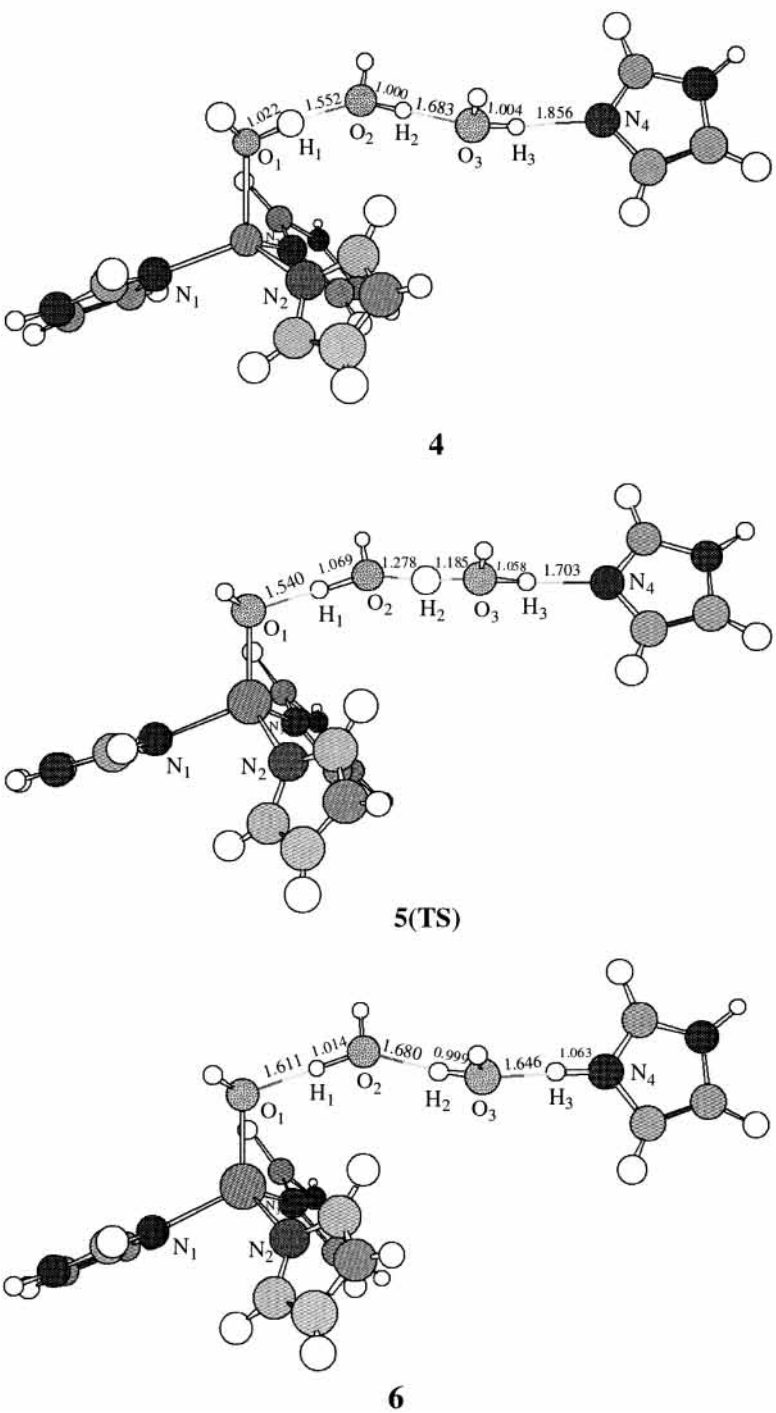

Figure 4. B3LYP-optimized structures related to the three-water model with the relative orientation of the terminal imidazole taken as determined in the X-ray structure.

or surrounding water molecules might form hydrogen bonds to the waters in the water bridge and thus affect the PT energy surface. To probe this effect, we add two side waters to the water chain of the model system to form a new model system (called the five-water model). With this model and without any geometric restrictions, our optimizations produce an intermediate corresponding to a $(Im)_3-Zn-OH-H_2O-H_3O-Im$ compound, a TS connecting the initial zinc-bound water species to the intermediate, and a TS between the intermediate and the PT product with the protonated imidazole (His64) group. The geometries of all these five species (**7**−**11**, respectively) are shown in Figure 5. The reactant **7** and product **11** have structures very similar to the corresponding species obtained in the freely optimized three-water model, except that each bridged water molecule is hydrogen bonded to one side water in these two species. A common feature of all five of these species is that the hydrogen bond interaction between two neighboring water molecules in the water chain is considerably stronger than that between a side water and a bridged water, as reflected in the calculated O···H−O bond distances. One question to be answered is why only one intermediate exists in the proton transfer potential energy surface. According to the step-by-step proton transfer mechanism, besides the intermediate **9**, it seems to us that another intermediate, $(Im)_3-Zn-OH-H_3O-H_2O-Im$, should exist. A plausible explanation for missing this intermediate is that there are large electrostatic repulsions

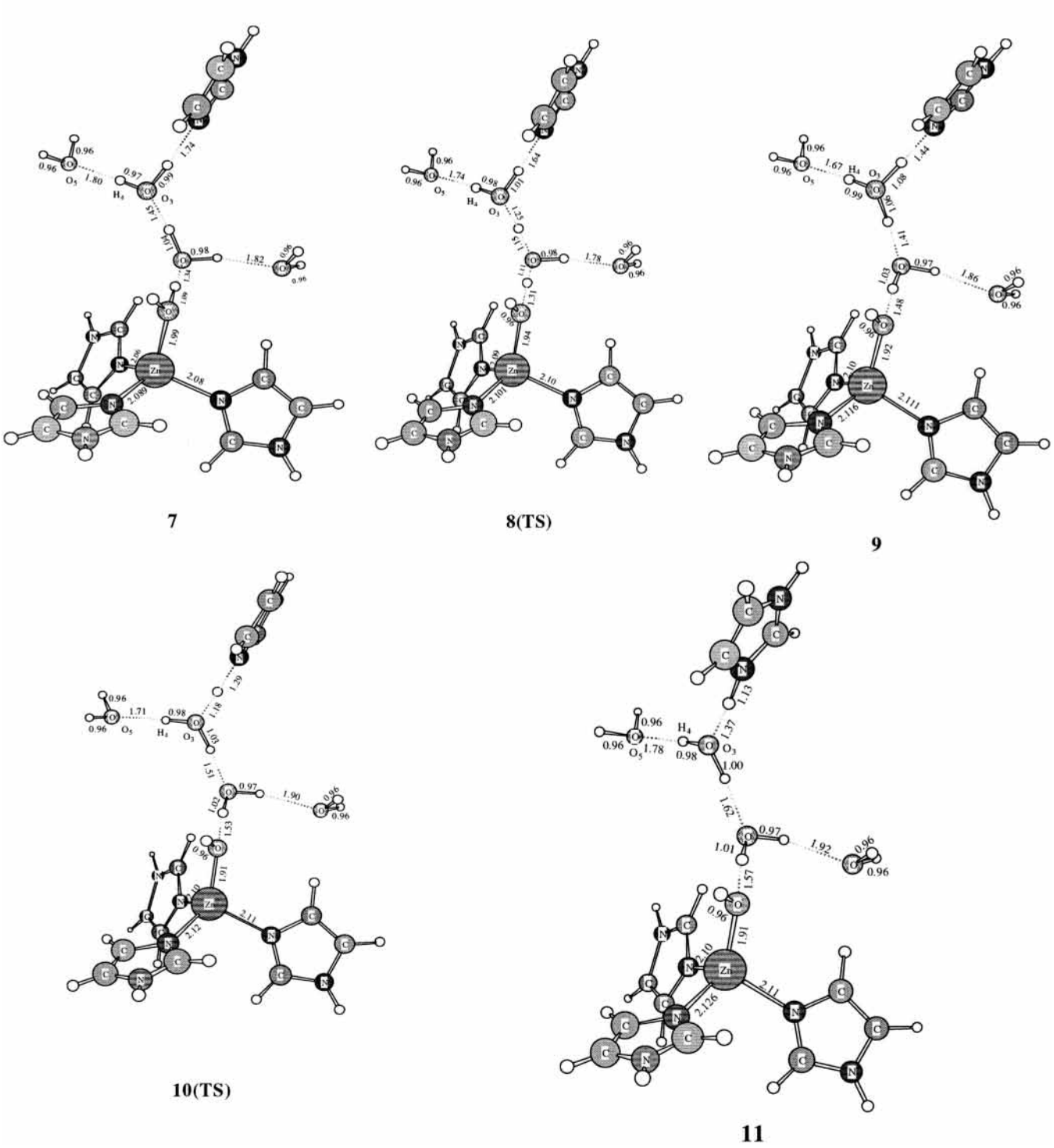

Figure 5. B3LYP-optimized structures related to the freely optimized five-water model.

between the zinc ion and its adjacent hydronium ion H_3O^+ to destabilize this hypothetical intermediate. Since the distance between H_3O^+ and Zn^{2+} in intermediate **9** is considerably larger than that in the hypothetical intermediate, intermediate **9** can be stabilized to exist with the help of the hydrogen bond interactions between the hydronium ion and its side water.

TS **8** represents one proton transfer from the zinc-bound water to the first bridge water and, at the same time, another proton transfer from the first bridge water to the second bridge water. Therefore, the first step from reactant **7** to intermediate **9** is concerted. The structure of TS **10** clearly indicates that the second step is a simple proton transfer from the protonated water (hydronium ion) to the imidazole acceptor. Thus, the calculations with the new model system and without geometry restrictions suggest that the proton transfer process involves two steps, a concerted proton transfer followed by a one-step proton transfer. The PT mechanism obtained here is dramatically different from that obtained in previous subsections, where a concerted PT process is favored.

The energies of **7**−**11** with and without ZPE corrections (calculated with basis set I) are collected in Table 2. As seen from the potential energy profile shown in Figure 6, the barrier is 1.46 kcal/mol for the first concerted PT process, and ∼0.60 kcal/mol for the second PT process. In the dehydration direction,

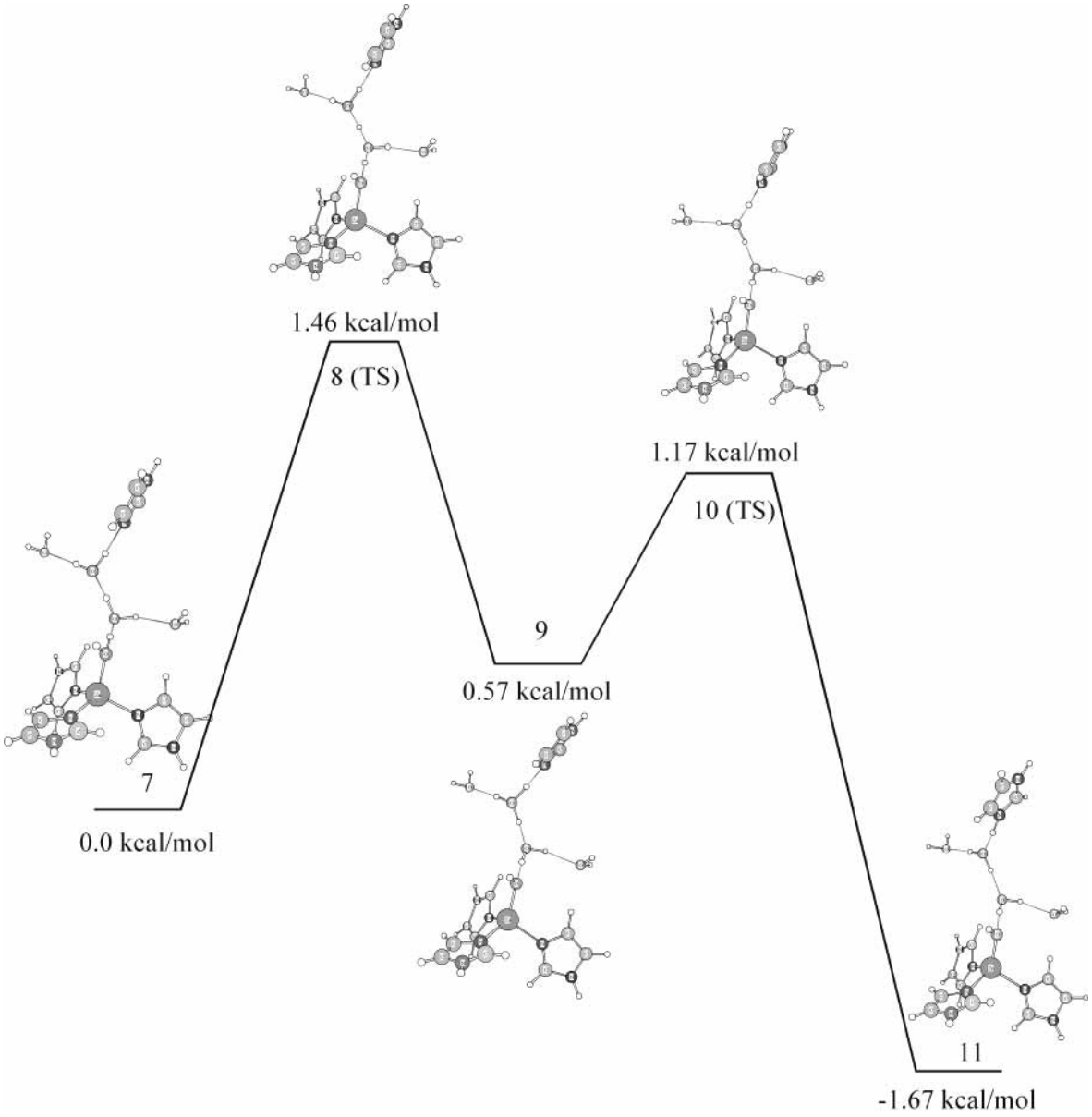

Figure 6. Potential energy profile of the five-water model.

TABLE 2: Relative Energies (kcal/mol) of Species 7−11 Related to the Freely Optimized Five-Water Model (ZPE Corrections Calculated with Basis Set I)

species	E_o	E_o + ZPE	species	E_o	E_o + ZPE
7	0.0	0.0	**10** (TS)	1.17	−0.56
8 (TS)	1.46	−0.72	**11**	−1.67	−1.75
9	0.57	−0.43			

the barrier is 2.84 kcal/mol for the first step and 0.89 kcal/mol for the second concerted PT step. Similar to that in the freely optimized three-water model, the inclusion of ZPE corrections makes transition states **8** and **10** slightly lower in energy than the intermediate or the reactant, indicating that the whole PT process in the hydration direction may be spontaneous.

Obviously, the PT barriers obtained above from the freely optimized five-water model do not agree with the experimental results. It could be expected that the geometrical constraints such as the D−A distance and the relative orientation of the terminal imidazole imposed by the protein backbone have a similar effect on the PT energy surface of the current model, as observed in the preceding subsections for the three-water model. Thus, we will not investigate these effects for the current model. Instead, we want to know whether the PT picture will change if the strength of the hydrogen bond between the side water and the bridged water is adjusted. The background of this study has two aspects. One is that the hydrogen bond interaction between the protein residues and the waters in the water shuttle may not be as strong as that simulated here by freely placing two side waters next to bridged waters one by one. Another is that the most frequently appearing water bridge between the Zn^{2+} ion and the His64 group is composed of three waters, as revealed from molecular dynamics studies[35] on CA.

By analyzing the structures of five species from the freely optimized five-water model, we notice that the quite strong hydrogen bond between the side water and the bridged water next to the terminal imidazole, as indicated by a relatively short $O_5\cdots H_4-O_3$ distance in Figure 5, is crucial for the stabilization of the hydronium ion in intermediate **9**. In contrast, the other side water is more like a spectator in the PT process. Hence, to study how the hydrogen bond between the side water and the bridged water affects the PT picture, we froze the distance $R(O_5-H_4)$ at 1.80 Å and allowed all other freedoms to be optimized. Interestingly, intermediate **9** is not a minimum again

in our partial optimizations, and thus, the PT mechanism should change to a concerted picture, analogous to what we obtained in preceding subsections. This result indicates that if two side waters or any other nearby residues are not strongly bonded to the waters in the water bridge the proton transfer may still occur in a concerted way. Of course, in this case two side waters may still play some secondary role in affecting the PT barriers in both directions.

4. Conclusions

In this work, we have performed B3LYP calculations with a minimum realistic model, $(Im_3)_3Zn^{2+}\cdots(OH_2)_3\cdots Im$, to investigate the intramolecular PT process in the active site of CA. With this three-water model, we have studied the PT barrier and mechanism under three circumstances: (a) without geometric restrictions, (b) with the proton donor−acceptor distance fixed, and (c) with the relative orientation of the imidazole acceptor fixed. The latter two circumstances are invoked to mimic the effect of the protein framework on the structure of the model system and thus on the PT energy surface. Our calculations demonstrate that under all three of these conditions the intramolecular PT process involves a concerted motion of three protons, but the PT barrier in either the hydration or dehydration direction varies considerably. If the proton donor−acceptor distance and the relative orientation of the imidazole acceptor are taken to be like those determined in the X-ray structure, the calculated PT barriers are 13.4 kcal/mol in the hydration direction and 13.2 kcal/mol in the dehydration direction. Further considerations of the protein electrostatic environment and zero-point vibrational energies lead to a reasonable estimate of ∼7 kcal/mol for the PT barrier in both directions, which are in good agreement with experimental values.

In addition, the effect of the nearby residues or surrounding water molecules on the PT energy surface is investigated by using a five-water model. Calculations have shown that with the freely optimized five-water model the proton transfer from the zinc-bound water to the imidazole acceptor involves a concerted motion of two protons followed by a one-step transfer of one proton, which is energetically spontaneous. Thus, the existence of a strong hydrogen bond network formed by the protein residues in the active site might change the overall mechanism of the intramolecular PT in the CA system. However, if the hydrogen bond interaction between the side water (or any other residue) and the water in the water chain is not sufficiently strong, the proton transfer still occurs in a concerted way. As revealed by the X-ray structure[3] and molecular dynamics studies,[35] there is no obvious evidence that the water bridge of the real enzyme CA could form such a strong hydrogen bond network with the nearby residues or surrounding water molecules. Thus, the calculations presented here tend to support the idea that the intramolecular PT process in the active site of CA is most likely concerted. On the other hand, we would like to point out that the stochastic and dynamically fluctuating environment of the real enzyme active site would make the concerted hopping of protons less likely than the present study suggests.

Acknowledgment. Part of the calculations was carried out on SGI Origin 3800 and Dawning 3000A instruments at Nanjing University. This work was supported by the National Natural Science Foundation of China (Grant 20073020).

References and Notes

(1) Stadie, W. C.; O'Brien, H. *J. Biol. Chem.* **1933**, *103*, 521−529.
(2) Tashian, R. E. *BioEssays* **1989**, *10*, 186−192.
(3) Eriksson, A. E.; Jones, T. A.; Liljas, A. *Proteins: Struct., Funct., Genet.* **1988**, *4*, 274.
(4) Silverman, D. N.; Tu, C. K.; Linskog, S.; Wynns, G. C. *J. Am. Chem. Soc.* **1979**, *101*, 6734.
(5) Tu, C. K.; Silverman, D. N. *J. Am. Chem. Soc.* **1975**, *97*, 5935.
(6) Lindskog, S.; Behravan, G.; Engstrant, C.; Forsman, C.; Jonsson, B.; Liang, Z.; Ren, X.; Xue, Y. In *Carbonic Anhydrase: From Biochemistry and Genetics to Physiology and Clinical Medicine*; Lindskog, S., Behravan, G., Engstrant, C., Forsman, C., Jonsson, B., Liang, Z., Ren, X., Xue, Y., Eds.; Wiley: Weinheim, Germany, 1991; pp 1−13.
(7) Silverman, D. N.; Linskog, S. *Acc. Chem. Res.* **1988**, *21*, 30.
(8) Venkatasubban, K. S.; Silverman, D. N. *Biochemistry* **1980**, *19*, 4984.
(9) Lesburg, C. A.; Christianson, D. W. *J. Am. Chem. Soc*. **1995**, 117, 6838.
(10) Lippard, S. J.; Berg, J. M. *Principles of Bioinorganic Chemistry*; University Science: Sausalito, CA, 1994; pp 257−281.
(11) Earnhardt, J. N.; Silverman, D. N. In *Comprehensive Biological Catalysis*; Sinnott, M., Ed.; Academic Press: San Diego, 1998; pp 483−506.
(12) Christianson, D. W.; Fierke, C. A. *Acc. Chem. Res.* **1996**, *29*, 331−339.
(13) Steiner, H.; Jonsson, B. H.; Linskog, S. *Eur. J. Biochem*. **1975**, *59*, 253.
(14) Pocker, Y.; Bjorkquist, D. W. *Biochemistry* **1977**, *16*, 5698.
(15) Tu, C. K.; Silverman, D. N. *Biochemistry* **1985**, *24*, 5881.
(16) Silverman, D. N.; Tu, C. K.; Chen, X.; Tanhouser, S. M.; Kresge, A. J.; Laipis, P. J. *Biochemistry* **1993**, *32*, 10757.
(17) Fierke, C. A.; Calderone, T. L.; Krebs, J. F. *Biochemistry* **1991**, *30*, 11054.
(18) Kiefer, L. L.; Paterno, S. A.; Fierke, C. A. *J. Am. Chem. Soc*. **1995**, *117*, 6831.
(19) Ghannam, A. F.; Tsen, W.; Rowlett, R. S. *J. Biol. Chem.* **1986**, *261*, 1164.
(20) Nair, S. K.; Christianson, D. W. *J. Am. Chem. Soc*. **1991**, *113*, 9455.
(21) Tu, C. K.; Wynns, G. C.; Silverman, D. N. *J. Biol. Chem.* **1981**, *256*, 9466.
(22) Liang, J.; Lipscomb, W. N. *J. Am. Chem. Soc*. **1986**, *108*, 5051.
(23) Liang, J.; Lipscomb, W. N. *Int. J. Quantum Chem*. **1989**, *36*, 299.
(24) Jacob, O.; Cardenas, R.; Tapia, O. *J. Am. Chem. Soc*. **1990**, *112*, 8692.
(25) Jacob, O.; Tapia, O. *Int. J. Quantum Chem.* **1992**, *42*, 1271.
(26) Merz, K. M., Jr.; Hoffmann, R.; Dewar, M. J. S. *J. Am. Chem. Soc.* **1989**, *111*, 5636−5649.
(27) Merz, K. M., Jr. *J. Am. Chem. Soc*. **1990**, *112*, 7973.
(28) Merz, K. M., Jr. *J. Am. Chem. Soc.* **1991**, *113*, 3572.
(29) Aqvist, A.; Warshel, A. *J. Mol. Biol.* **1992**, *224*, 7.
(30) Demoulin, D.; Pullman, A. *Theor. Chim. Acta* **1978**, *49*, 161.
(31) Pullman, A.; Demoulin, D. *Int. J. Quantum Chem.* **1979**, *16*, 641.
(32) Lu, D.; Voth, G. *J. Am. Chem. Soc.* **1998**, *120*, 4006−4014.
(33) Sheridan, R. P.; Allen, L. C. *J. Am. Chem. Soc*. **1981**, *103*, 1544.
(34) Isaev, A.; Scheiner, S. *J. Phys. Chem. B* **2001**, *105*, 6420.
(35) Lu, D.; Voth, G. *Proteins: Struct., Funct., Genet.* **1998**, *33*, 119.
(36) Levine, I. R. In *Quantum Chemistry*, 5th ed.; Prentice Hall: Upper Saddle River, NJ, 2000.
(37) Frisch, M. J.; Trucks, G. W.; Schlegel, H. B.; Scuseria, G. E.; Robb, M. A.; Cheeseman, J. R.; Zakrzewski, V. G.; Montgomery, J. A., Jr.; Stratmann, R. E.; Burant, J. C.; Dapprich, S.; Millam, J. M.; Daniels, A. D.; Kudin, K. N.; Strain, M. C.; Farkas, O.; Tomasi, J.; Barone, V.; Cossi, M.; Cammi, R.; Mennucci, B.; Pomelli, C.; Adamo, C.; Clifford, S.; Ochterski, J.; Petersson, G. A.; Ayala, P. Y.; Cui, Q.; Morokuma, K.; Malick, D. K.; Rabuck, A. D.; Raghavachari, K.; Foresman, J. B.; Cioslowski, J.; Ortiz, J. V.; Baboul, A. G.; Stefanov, B. B.; Liu, G.; Liashenko, A.; Piskorz, P.; Komaromi, I.; Gomperts, R.; Martin, R. L.; Fox, D. J.; Keith, T.; Al-Laham, M. A.; Peng, C. Y.; Nanayakkara, A.; Challacombe, M.;Gill, P. M. W.; Johnson, B.; Chen, W.; Wong, M. W.; Andres, J. L.; Gonzalez, C.; Head-Gordon, M.; Replogle, E. S.; Pople, J. A. *Gaussian 98*, revision A.9; Gaussian, Inc.: Pittsburgh, PA, 1998.
(38) Ehler, A. W.; Böhme, M.; Dapprich, S.; Gobbi, A.; Höllwarth, A.; Jonas, V.; Köhler, K. F.; Stegmann, R.; Velkamp, A.; Frenking, G. *Chem. Phys. Lett.* **1993**, *208*, 111.
(39) Couty, M.; Hall, M. B. *J. Comput. Chem.* **1996**, *17*, 1359.
(40) Branko, S. J. *THEOCHEM* **1997**, *417*, 89−94.